Journal of Computational Physics 228 (2009) 1343–1346

Contents lists available at ScienceDirect

Journal of Computational Physics

journal homepage: www.elsevier.com/locate/jcp

Short Note

Multi-dimensional dissipation for cure of pathological behaviors of upwind scheme

Ching Y. Loh *, Philip C.E. Jorgenson

NASA Glenn Research Center at Lewis Field, 21000 Brookpark Road, Cleveland, OH 44135, United States

ARTICLE INFO

Article history:
Received 22 September 2008
Accepted 29 October 2008
Available online 18 November 2008

Keywords:
Compressible flow
Upwind finite volume scheme
Pathological behaviors
Multi-dimensional dissipation

1. The pathological behaviors of upwind scheme

Upwind finite volume (FV) schemes are broadly used in computational fluid dynamics (CFD) primarily due to their robustness and geometric flexibility. However, despite their great success, there are still some cases of failure reported by researchers. For example, the carbuncle phenomenon, the expansion shock, and the numerical oscillation across a slow moving shock, etc. [2–4]. It is generally agreed that insufficient dissipation and the consequent local numerical instability lead to such failures [1,3,4]. To stabilize the Godunov type upwind schemes, various ways of adding dissipation were suggested. Quirk [3] used a more dissipative HLLE Riemann solver and Lin [5] provides a way to add dissipation to FDS (flux difference splitting) schemes to treat some of the pathological behaviors. Recently, Xu [1,2] investigated the numerical dissipation and further argued that for a Godunov type upwind scheme:

- The dissipation required by the numerical stability mainly comes from the Riemann solver at the cell interface. With the given L (left) and R (right) states across the cell interface, the Riemann solver compromises the two different states to an intermediate state for the flux by some kind of averaging, leading to entropy increase and numerical dissipation is generated.
- The amount of dissipation varies subject to the L and R states and occurs *only* in the direction *normal* to the cell interface. The more they differ from each other, the more the numerical dissipation. In the direction *tangent* to the surface, the numerical dissipation is absent.

* Corresponding author. Tel.: +1 216 433 3981; fax: +1 216 433 5802.
E-mail address: Ching.Y.Loh@grc.nasa.gov (C.Y. Loh).

0021-9991/$ - see front matter
doi:10.1016/j.jcp.2008.10.044

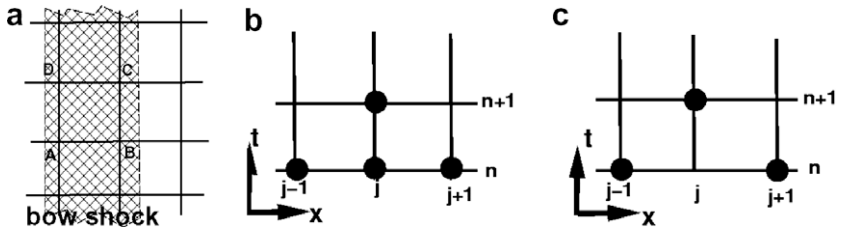

Fig. 1. (a) Numerical dissipation in a bow shock, (b) grid for an unconditionally unstable scheme, and (c) grid for the Lax–Friedrichs scheme.

For the carbuncle phenomenon, as shown in Fig. 1(a), we assume a rectangular grid and that the grid lines *AD* and *BC* are aligned with the bow shock. Based on Xu's argument, as the flow states jump sharply across *BC* (or *AD*) due to the bow shock, the Riemann solver (RS) at *BC* introduces numerical dissipation in the *normal* direction. As for the surface *CD* (or *AB*), since the *L* and *R* states are almost identical, the RS provides little or no dissipation in its normal direction. Thus, the numerical solution is vulnerable to the local temporal or spatial instabilities in the direction tangent to the shock, which causes the carbuncle phenomenon. A natural remedy is to add some extra numerical dissipation in the *tangential* direction.

On the other hand, the expansion shock represents a different type of pathological behavior with insufficient dissipation in the direction *normal* to the cell interface (Fig. 3(a)). Quirk [3] suggested using a more dissipative HLLE RS and smearing the "expansion shock" to an expansion fan.

For *systematic cure* of the pathological behaviors, based on the above qualitative analysis, we propose here a simple *multi-dimensional dissipation* model that is external to the RS. The model adds omni-directional dissipation to the upwind scheme, and can be easily implemented.

2. The multi-dimensional dissipation model

A sample one-dimensional dissipation model: To explain how the dissipation model works, we begin with a simple one-dimensional scalar advection equation $\frac{\partial u}{\partial t}+\frac{\partial u}{\partial x}=0$. Two schemes are reviewed. The first one is an unstable scheme with forward difference in time and central difference in space (Fig. 1(b))

$$u_j^{n+1}=u_j^n+0.5r(u_{j+1}^n-u_{j-1}^n),$$

where $r=\Delta t/\Delta x$. However, if u_j^n is replaced by an average of u at the adjacent points, $u_{avg}=0.5(u_{j+1}^n+u_{j-1}^n)$, the scheme becomes the Lax–Friedrichs scheme (Fig. 1(c)), which is stable for $r\leqslant 1$. Here, we have learned that when replacing u_j^n by an average of u at the adjacent nodes, a certain amount of dissipation is added to the scheme, turning it to a stable one. This simple idea will be used to construct the following multi-dimensional dissipation model.

The multi-dimensional dissipation model: Now, consider the (vector) solution $\mathbf{U}_j^n$ of the two-dimensional Euler equations in conservation form:

$$\mathbf{U}_t+\mathbf{F}_x+\mathbf{G}_y=\mathbf{0}. \tag{1}$$

For the dissipation model, $\widetilde{\mathbf{U}}=\mathbf{U}_{avg}$ can be obtained by averaging $\mathbf{U}^n$ at time step n at the cell interface centers (mid-points) M,N,P,Q. They are the R states for RS extrapolated from their corresponding neighboring cell centers (Fig. 2). Respectively, for triangular and rectangular cells,

$$\widetilde{\mathbf{U}}=(\mathbf{U}_M^n+\mathbf{U}_N^n+\mathbf{U}_P^n)/3,\quad \text{or}\quad \widetilde{\mathbf{U}}=(\mathbf{U}_M^n+\mathbf{U}_N^n+\mathbf{U}_P^n+\mathbf{U}_Q^n)/4.$$

For an upwind FV scheme, the multi-dimensional dissipation model is introduced by simply replacing $\mathbf{U}^n$ with a weighted average $\beta\widetilde{\mathbf{U}}+(1-\beta)\mathbf{U}^n$ where β, $0\leqslant\beta<1$, is the weighing factor for dissipation control. For example, here is the scheme with triangular grid for Eq. (1):

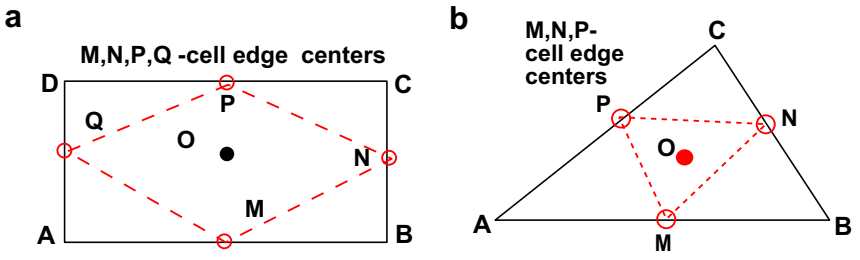

Fig. 2. Dissipation models in 2D spaces: (a) for rectangular cell, (b) for triangular cell; O is the cell center, M,N,P,Q are the cell edge centers for the averaged $\widetilde{\mathbf{U}}$.

$$\mathbf{U}^{n+1} = \beta\widetilde{\mathbf{U}} + (1-\beta)\mathbf{U}^{n} - \frac{\Delta t}{\Delta s}\sum_{k=1}^{3}\left[\mathbf{F}_{k}^{n+1/2}(n_x)_k + \mathbf{G}_{k}^{n+1/2}(n_y)_k\right]\Delta l_k, \tag{2}$$

where $\Delta s, \Delta l_k, (n_x, n_y)$ are, respectively the cell area, cell edge length and out-going unit normal vectors at each cell edge k. Most subsonic or low supersonic flows are insensitive and resilient to β. With the upwind scheme we use [6], $\beta = 10^{-3}$ is a reasonable choice. For flows with extremely high Mach number and strong shocks, β may need to increase up to 0.3 or higher. To avoid excessive dissipation, one should keep β as small as possible.

3. Numerical examples for curing the pathological behaviors

- *The expansion shock:* Consider the problem of a strong shock diffracting over a 90° edge [3]. There are about 14,4000 triangular cells in the domain. Initially, the flow is set to the quiescent ambient condition: $(\rho_0, u_0, v_0, p_0) = (1, 0, 0, 1/\gamma)$, and $M_s = 5.09$ conditions are imposed at the inlet: $(\rho_i, u_i, v_i, p_i) = (5.0294, 4.0779, 0, 21.4710)$. At the top, bottom, and along the surfaces of the rectangular block, the slip wall condition is imposed. A simple extrapolation condition is applied to the outlet boundary. Fig. 3(a) and (b) show the density contours with or without the cure. With β changing slightly from 0 to 0.001, the expansion shock disappears.
- *The carbuncle phenomenon:* Consider a Mach $M = 10$ flow past a circle (blunt body). Slip condition is imposed on the solid wall. Simple extrapolation is applied to the outflow boundaries. There are about 80,000 triangular cells in the computational domain. As shown in Fig. 3(c) and (d), for a basic Godunov scheme ($\beta = 0$), the carbuncle phenomenon is prominent but disappears when a maximum $\beta = 0.05$ is applied.
- *The slowly moving shock:* A grid consisting of 800 uniform cells is used, spanning between $0 \leqslant x \leqslant 32$. Initially, a strong shock is located at $x = 15$ with the left states $(\rho_l, u_l, p_l) = (3.86, 0.81, 10.34)$ and the right states $(\rho_r, u_r, p_r) = (1, 3.44, 1)$. These states are also imposed as the inflow and outflow boundary conditions. Fig. 4 shows that by increasing β from 0 to 0.3 and 0.5, the spurious oscillation is suppressed.

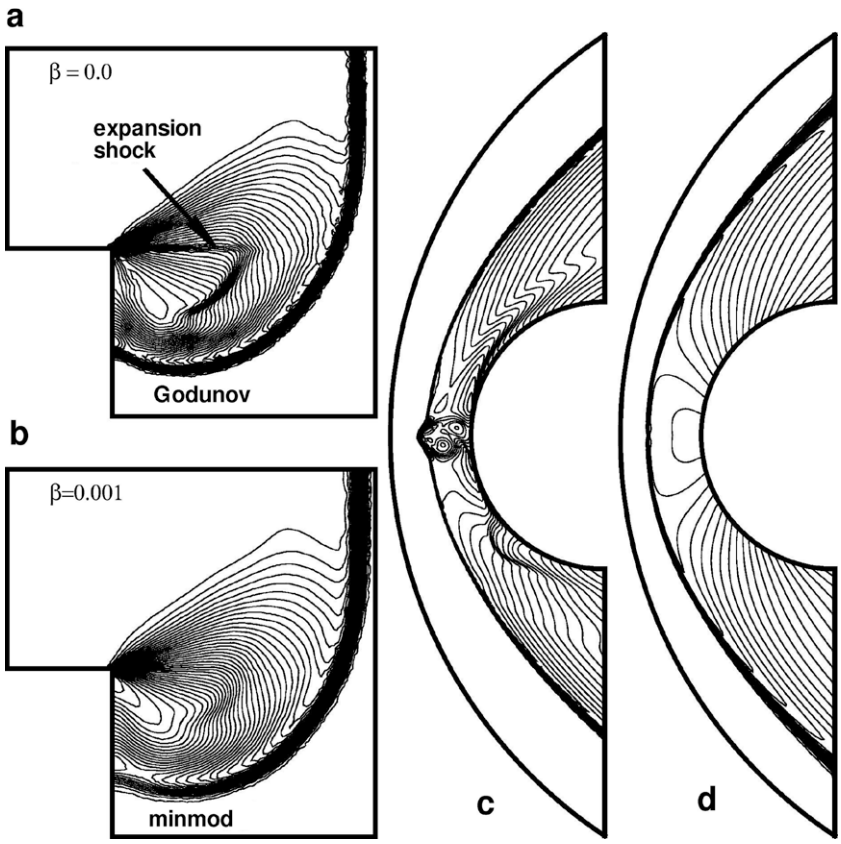

Fig. 3. (a) Supersonic $M = 5.09$ flow over a 90° edge, showing an "expansion shock"; (b) with $\beta = 0.001$, the expansion shock disappears (a minmod limiter is used with a Godunov type scheme); (c) Supersonic $M = 10$ flow past a circular blunt body, showing carbuncle phenomenon with Godunov scheme ($\beta = 0$); and (d) with maximum $\beta = 0.05$ imposed, the carbuncle phenomenon disappears.

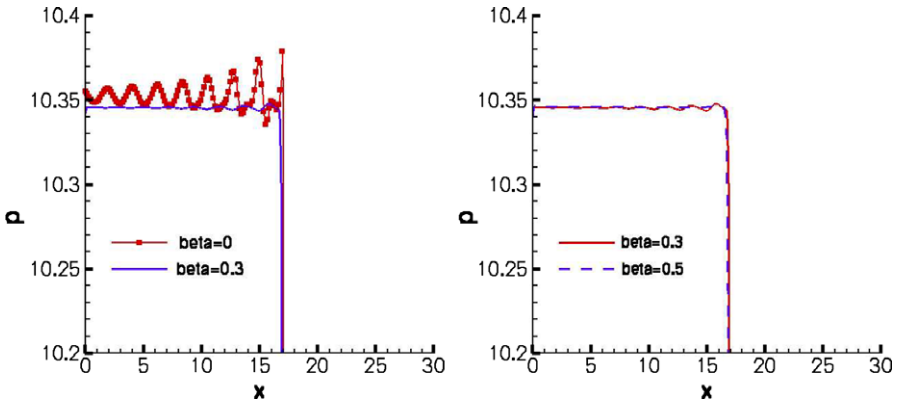

Fig. 4. Suppression of spurious oscillation in one-dimensional slowly moving shock at $t = 20$ (10,000 steps); left: comparison for $\beta = 0$ and $\beta = 0.3$; right: comparison for $\beta = 0.3$ and $\beta = 0.5$, shows growing numerical dissipation with increased β.

References

[1] K. Xu, Z. Li, Dissipative mechanism in Godunov-type schemes, Int. J. Numer. Meth. Fluid 37 (2001) 1–22.
[2] K. Xu, A gas-kinetic BGK scheme for the Navier–Stokes equations and its connection with artificial dissipation and Godunov method, J. Comput. Phys. 171 (2001) 289–335.
[3] J.J. Quirk, A contribution to the great Riemann solver debate, Int. J. Num. Meth. Fluid 18 (1994) 555–574.
[4] J. Gressier, J.-M. Mosshetta, On the pathological behavior of upwind schemes, AIAA Paper 98-0110, 1998.
[5] H.C. Lin, Dissipation additions to flux difference splitting, J. Comput. Phys. 117 (1) (1995) 20–27.
[6] C.Y. Loh, P.C.E. Jorgenson, A time accurate upwind unstructured finite volume method for compressible flow with cure of pathological behaviors, AIAA Paper 2007-4463, 2007.